Plasma Chem Plasma Process (2011) 31:417–426
DOI 10.1007/s11090-011-9296-1

ORIGINAL PAPER

Time-Resolved Fourier Transform Emission Spectroscopy of CF_3Br and CF_3CFHCF_3 in a Pulsed Electrical Discharge

Martin Ferus · Svatopluk Civiš · Petr Kubelík · Václav Nevrlý · Petr Bitala · Eva Grigorová · Michal Střižík · Pavel Kubát · Zdeněk Zelinger

Received: 21 November 2010 / Accepted: 22 March 2011 / Published online: 9 April 2011

Abstract The environmentally important decomposition of halogenated species CF_3Br and CF_3CHFCF_3 in helium discharge plasma was investigated by time-resolved high-resolution Fourier transform infrared emission spectroscopy. Contrary to classical pyrolysis, a deeper fragmentation of precursors up to atoms and lower molecular species was observed. Excited molecular products CF, CF_2 and CF_4 achieved the maximal concentration in the afterglow. The high concentration of all these species is in agreement with a kinetic model based on radical chemistry. The non-detectable concentration of CF_3 can be connected to its high reactivity and the formation of more stable products, CF_4 and CF_2, by addition or release of a fluorine atom, respectively. Other products included HF, HBr, CO and cyano compounds that were produced by secondary reactions with traces of water vapor, atmospheric oxygen and nitrogen present in original industrial samples as impurities.

Keywords Helium discharge plasma · CF_3Br · CF_3CHFCF_3 · Fluorocarbon radicals · Time-resolved FTIR

Introduction

Halogenated fire extinguishing agents have been traditionally utilized in many applications to protect fixed enclosures or in applications requiring rapid extinguishing. The most commonly used halogenated hydrocarbon extinguishing agents were bromine-containing

M. Ferus · S. Civiš · P. Kubelík · P. Kubát · Z. Zelinger (✉)
J. Heyrovský Institute of Physical Chemistry, v.v.i., Academy of Sciences of the Czech Republic, Dolejškova 3, 18223 Prague 8, Czech Republic
e-mail: zelinger@jh-inst.cas.cz

M. Ferus · P. Kubelík
Institute of Physics, v.v.i., Academy of Sciences of the Czech Republic, Na Slovance 2, 18221 Prague 8, Czech Republic

V. Nevrlý · P. Bitala · E. Grigorová · M. Střižík
VŠB—Technical University of Ostrava, Faculty of Safety Engineering, Lumírova 13, 70030 Ostrava—Výškovice, Czech Republic

compounds, e.g., CF_3Br (Halon^{TM} 1301). The Montreal Protocol and its attendant amendments have mandated that their production be discontinued [1] because these compounds have been linked to the ozone depletion [2, 3] and to the formation of toxic products [4, 5]. Nonbrominated fluorohydrocarbons [6], e.g., CF_3CHFCF_3 are suitable alternatives of growing importance for both fixed and portable fire extinguishing systems. The behavior of these agents in thermal and non-thermal plasma as well as related environmental aspects and their decomposition products are still challenging tasks in the context of fire safety science.

In previous papers, high resolution spectroscopic studies of halogenated radicals were performed [7–10], and time-resolved high-resolution Fourier transform infrared (FTIR) spectroscopy was used to study plasma processes in an electrical discharge [11, 12] and/or in a plasma plume formed by laser ablation of various materials [13, 14]. Although the time-resolved spectroscopy can significantly contribute to the better understanding of the processes, so far, no study has been published on the measurement of time resolved spectra of the decomposition products of CF_3Br or CF_3CHFCF_3. Because of the high stability of fluorohydrocarbons, pulsed helium discharge plasma was used, which allows the generation of the high concentration of unstable species that is expected to occur at moderate temperatures with low yields but at conditions far from the thermal equilibrium with excitation temperature of about 3,500 K [15]. Non-thermal fluorocarbon plasma serves as an effective source of high-energy electrons and chemically active particles with applications in material science, where it is widely used for etching semiconductors [16, 17].

The time-resolved data provide more detailed information about the kinetics of unstable species than the classical steady-state FTIR of fluorocarbons [18]. The high resolution (typically 0.05 cm^{-1}) can resolve lines of individual species in a wide spectral range, and the individual formation and decay processes can be studied simultaneously. The limitation of this method is the sensitivity of the FTIR emission technique (commonly at least about 10^9–10^{12} particles per cm^3) and the considerable time required to obtain the data because signal accumulation is necessary.

Experimental

The emission spectra were measured using a time-resolved Fourier transform high-resolution Bruker IFS 120 HR interferometer. The basic principle of this method, described in previous papers [11, 19] is the acquisition of signals from the detector during discharge pulses for different optical path differences. These signals are shifted in time by Δt (where $\Delta t = 1$, 2 or 3 μs). In this way, a matrix $I(t_{k,}\ \delta_i)$ of intensity I at times t_k is acquired for the given optical path difference δi (i is the index of the selected optical path difference, from its zero to maximum values). This process results in 30 to 64 reciprocally time-shifted interferograms computed as a spectrum using the Fourier transformation.

The scheme of experimental set-up is depicted in Fig. 1. The positive column discharge tube, covered with a glass outer jacket, was 25 cm long with an inner diameter of 12 mm. KBr windows were used. The pulsed discharge was maintained by a high voltage transistor switch HTS 81 (Behlke electronic GmbH, Frankfurt, Germany) and applied between the stainless steel anode and the grounded cathode.

The He/precursor plasma was cooled by water in the outer jacket of the cell. The voltage drop across the discharge was 1,200 V, with a pulse width of 20 μs and 0.6 A peak-to-peak current. The scanner velocity of FTS was set to produce a 5 or 10 kHz HeNe laser fringe frequency, which was used to trigger the discharge pulse. The recorded spectral

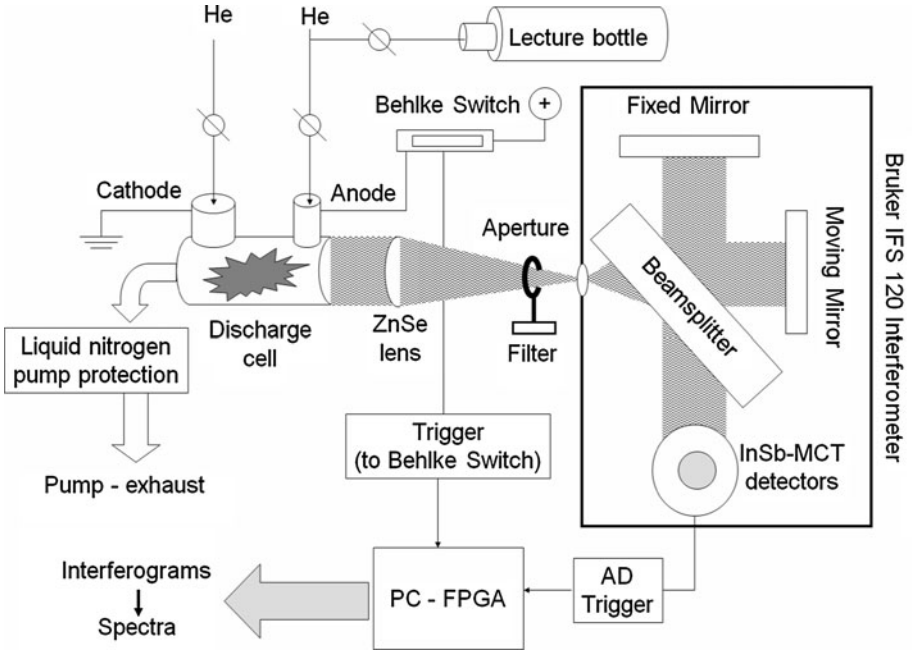

Fig. 1 Experimental set-up

range was 600–2,000 cm^{-1} and 2,000–6,000 cm^{-1} using a ZnSe lens and a series of Ge optical filters at an unapodized resolution of 0.05 cm^{-1}. This spectral range is very wide, commonly only one of these spectral regions is measured. Fifty scans were averaged to obtain a reasonable signal-to-noise ratio. The signal was detected by MCT and InSb detectors. Samples from the industry reservoir that contain air impurities (oxygen, moisture) were taken to the small lecture bottle at a pressure of 8 atm. The initial pressure of the extinguish agent, 0.5 mbar, was sampled from the lecture bottle, and the He buffer gas (99.999% purity) at a pressure in the range 2–4 mbar was co-added to obtain a stable glow discharge. Discharge products were pumped-out from the cell by the rotational pump (Edwards) after each pulse, and the He/precursor system was continually refreshed.

Results and Discussion

FTIR Emission Spectra

The FTIR spectra of He/C_3F_7H and He/CF_3Br mixtures in pulsed discharge are shown in Figs. 2 and 3, respectively.

Among the many atomic transitions of excited He* in the IR region, the strongest lines were assigned to the He I (e.g. ^3S-$^3P^o$ line 918.92 cm^{-1} $\sim$ 23.7 eV), system of transitions at 2,469.75 cm^{-1}, He I $^3P^o$-^3D (line 2,700.09 cm^{-1} $\sim$ 24.0 eV) or very strong He I ^1S-$^1P^o$ (line 4,857.46 cm^{-1} $\sim$ 21.2 eV). Energies in brackets corresponding to the upper level of given transitions show that electrons with energies close to the first ionization energy of He (24.58 eV) are available due to Penning ionization. However, He II was not detected,

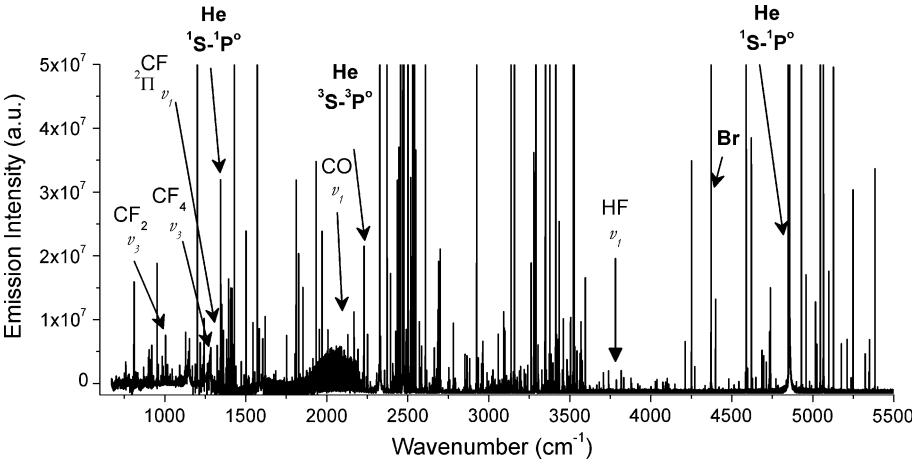

Fig. 2 FTIR spectrum (600–5,500 cm^{-1}) observed for He/CF_3Br mixture in a pulsed discharge

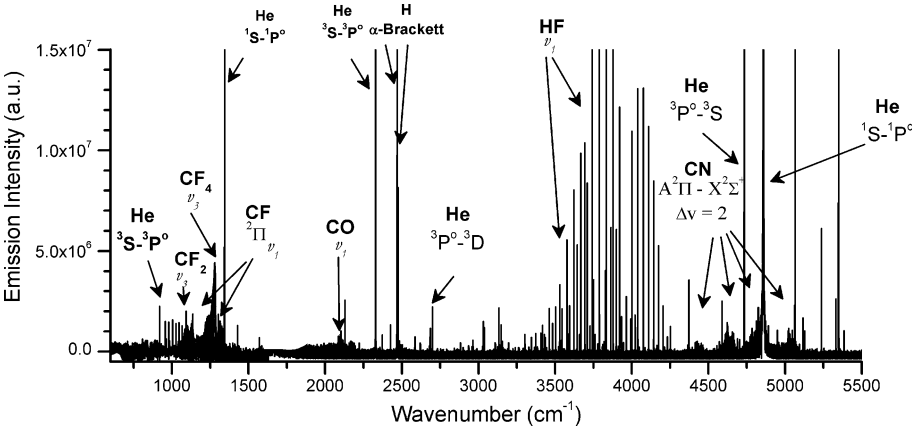

Fig. 3 FTIR spectrum (600 –5,500 cm^{-1}) observed for He/CF_3CHFCF_3 mixture in a pulsed discharge

which is in agreement with the observed electron energy distribution in helium discharge [20], where the energy continuously decreases into area of the first ionization potentials with an energy maximum of several electron volts.

The lines of atomic hydrogen H I (α-Brackett series at 2,467.73 cm^{-1} ~ 13.0 eV) for CF_3CHFCF_3 and atomic bromine Br I (e.g., transitions at 4,372.07 cm^{-1}) for CF_3Br were observed as well. Surprisingly, a low intensity was observed at the atomic lines of carbon, and the strongest line at 2,963.984 cm^{-1} was assigned to the ^{3}D-^{3}F^o transition. The atomic spectrum of fluorine F I in the IR region has not been studied before. The data were calculated on the basis of the extrapolation of results in the visible spectral region; [21] however, the lines of F I in the FTIR spectra of both compounds cannot be assigned due to their low intensity and/or overlapping with other lines.

The molecular species formed in the helium discharge plasma include predominantly the decomposition products of CF_3Br and CF_3CHFCF_3, namely HBr (ν_1 band at 2,558 cm^{-1}, Fig. 2), HF (ν_1 band at 3,962 cm^{-1}, Figs. 2 and 3), CF (P branch of $^2\Pi_{1/2}$

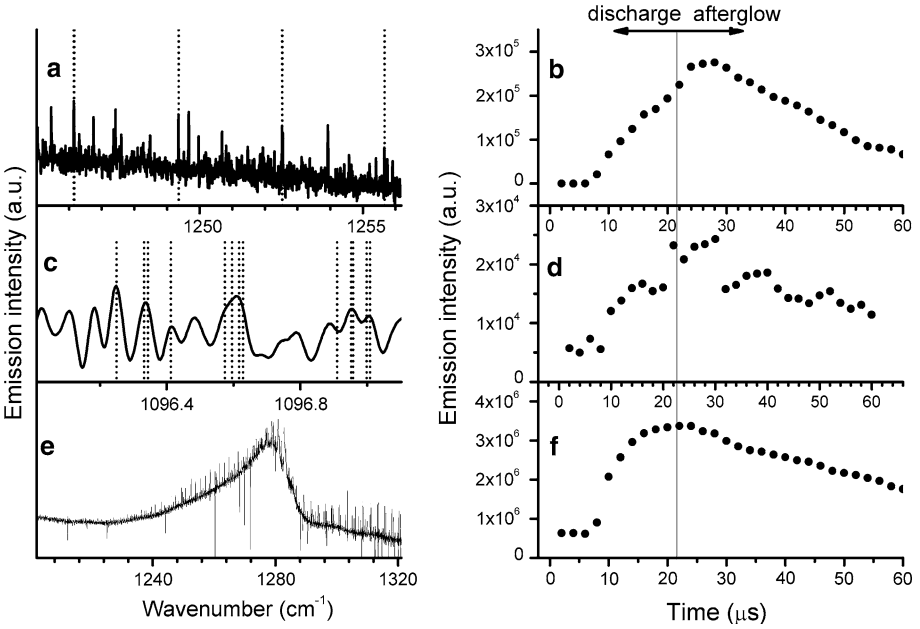

Fig. 4 Assignments of CF (**a**), CF_2 (**c**) and CF_4 (**e**) lines in high resolution FTIR spectra in He/CF_3CHFCF_3 discharge and their comparison with literature data (*dotted lines*). Corresponding time profiles of integrated intensities of CF $^2\Pi_{1/2}$ band (**b**), CF_2 v_3 band (**d**) and CF_4 v_3 band (**f**) are shown in the right side of this figure

band at 1,286 cm^{-1}, Fig. 4a) [22], CF_2 (P branch of v_3 band, Fig. 4c) [23, 24], and CF_4 (v_3 band at 1,281 cm^{-1}, Fig. 4e). Although the CF_3Br molecule does not contain hydrogen, HF was identified in the spectra of both CF_3Br and CF_3CHFCF_3 decomposition products, probably due to presence of water traces in industrial samples.

The lines of CF_3 radical [25] that can be expected in plasma discharge were not explicitly assigned due to congested spectra and possible overlap with lines of similar species, e.g., C_2F_6. The non-detectable concentration of CF_3 can be connected to its reactivity and the formation of more stable products, CF_4 and CF_2, by the addition or release of fluorine, respectively. No direct evidence of CF_3 formation is in agreement with results of the pyrolysis of CF_3CHFCF_3, where the most favored reaction is the elimination of HF at lower temperatures and the formation of CF_2 radicals at higher temperatures [26].

Lines of carbon monoxide CO at 2,143 cm^{-1} and the electronic transition $A^2\Pi$-$X^2\Sigma^+$ of the CN radical around 4,750 cm^{-1} (Figs. 2 and 3) were also found. The addition of water vapor to discharge led to the formation of HCN (v_1 band at 3,311 cm^{-1}). All these species are toxic, and their origin is in secondary reactions of reactive decomposition products in the discharge with air traces and/or water vapor, which are the main contaminants of industrial samples of fire extinguishing agents CF_3Br and CF_3CHFCF_3.

Kinetics and Chemical Processes in the Discharge

The use of time-resolved FTIR data (Figs. 3 and 4) permits a detailed description of the kinetics of the formation and decay of unstable species. The individual processes were studied in the wide spectral range of 600–6,000 cm^{-1}. These results provide information about the time profiles of the unstable species concentrations in excited states. The time

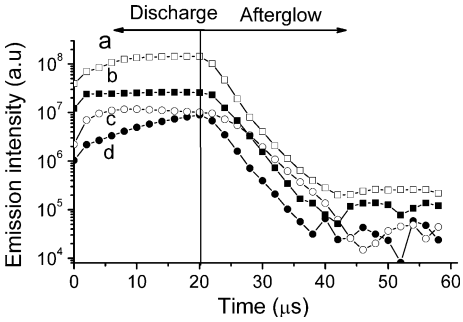

Fig. 5 Time resolved concentration profiles of atomic lines of Br (**a**), He (**b**), H (**c**), and C (**d**) observed for He/CF_3Br mixture in a pulse discharge

profiles show the difference between the deactivation of atoms (Fig. 5) and molecular species (Fig. 4b, d, f). Whereas atomic species deactivate spontaneously immediately after pulsed discharge with lifetime of several μs (Fig. 5), excited molecular species of CF (Fig. 4b), CF_2 (Fig. 4d) and CF_4 (Fig. 4f) achieve their maximal concentration in the afterglow. This observation could be connected to their formation from atoms and lower molecular fragments and/or deactivation from higher energy levels.

The emission profiles do not reflect the absolute total concentration of species, which are predominantly quenched to the ground state. Knowledge of the Einstein coefficients for spontaneous emission and bimolecular quenching rate constants is, therefore, essential for their quantification. The total concentrations of the species may be different from the concentration of excited species as forbidden transitions for the metastable levels, and radiation trapping for the resonant levels can change energy distribution inside individual species significantly.

Unstable species (ions, excited states) in helium discharge plasma are formed by Penning ionization (Eq. 1) and/or by molecular dissociation due to collisions with He* (Eq. 2) and electrons (Eq. 3): [27, 28]

$$AB + He* \rightarrow AB^+ + He + e^- \quad (1)$$

$$AB + He* \rightarrow A + B + He \quad (2)$$

$$AB + e^- \rightarrow A + B + e^- \quad (3)$$

He* represents a helium atom (metastable states 2^1S with energy of 20.6 eV and 2^3S with energy of 19.8 eV), and AB denotes a molecule with fragments A and B. In comparison with the lowest lying He (2^3S), the energies required for the ionization of CF_3Br (ionization potential of 11.4 eV) and CF_3CHFCF_3 (12.4 eV) are significantly lower [24].

The dissociation energy for the C-X bond decreases in the following order: C–F > C–H > C–C > C–Br [29]. The energies of excited He* atoms are significantly higher than the literature data for C–F bonds with the highest dissociation energy (E_{diss} <5.7 eV), and they allow simultaneous splitting of a few bonds during one collision with excited He* atoms and the formation of the observed CF and CF_2 fragments (Eq. 2). In reactions where multiple bonds are broken, the bond dissociation energy of a particular bond can be changed by the cleavage of ancillary bonds within the molecule. That is, once the first bond is broken, the remaining bond dissociation energies are often altered, e.g., the experimental values for C–F bonds are 5.31 eV (CF_4) [30], 4.00 eV (CF_3) [30], 4.59 eV (CF_2) [31], and 5.67 eV (CF) [32].

Electron impact data for both precursors (Eq. 3) are not available; however, similar studies with CF_3H and CF_4 were carried out. The minimal energy for hydrogen (Eq. 4) and

fluorine release (Eq. 6) was calculated to be 11 and 13 eV, respectively. The threshold energy for the direct formation of CH was found to be 19.5 eV. For comparison, the threshold energy of CF_4 dissociation to CF_3 and CF_2 fragments by electron impact was experimentally measured to be 12.5 eV with an optimum of 125 eV [33]. The highest effective cross-sections σ for an energy of 20 eV were observed for reactions (Eqs. 4–6) leading to the formation of CF and CF_3 radicals:[34]

$$CF_3H \rightarrow CF_3 + H \quad \sigma = 2 \times 10^{-22} m^2 \tag{4}$$

$$CF_3H \rightarrow CF + \text{other fragments} \quad \sigma = 1 \times 10^{-22} m^2 \tag{5}$$

$$CF_3H \rightarrow CHF_2 + F \quad \sigma = 1 \times 10^{-23} m^2 \tag{6}$$

In summary, the energetics of all processes described by Eqs. 4–6 show that both collisions with excited helium atoms and/or with fast electrons can be responsible for the deep fragmentation of CF_3Br and CF_3CHFCF_3.

Kinetic Model of CF_3Br Chemistry

A kinetic model of CF_3Br discharge and afterglow was designed on the basis of the reactions listed in Table 1. This model was presented in a previous paper [35] in detail, and it focuses on the radical chemistry because no ions were directly observed.

Briefly, the numerical model was implemented in the Python 2.6.4 programming language using the modules Numpy [36] and Scipy [37] as a zero-dimensional model describing only the time evolution of the concentrations. This type of model is appropriate for data originating from the homogeneous region of the positive column of a glow discharge. The activity of the discharge was simulated by a rectangular pulse with an electron number density of 22 μs in duration in accordance with the experiment. The typical values of electron densities in a glow discharge are between 10^9 and 10^{11} particles per cm^3 (ref [38, 39].). A value of 6×10^{11} particles per cm^3 obtained by a Langmuir probe measurement in the actual experimental discharge was used. The electron temperature not obtained by measurement was set as a free parameter in the range of 0.5–4 eV. The number densities of the precursor molecules were fixed at 6.58×10^{15} cm^{-3}, as calculated from their partial pressures of 50 Pa and the temperature of the glow discharge of 550 K. The temperature was obtained from a Boltzmann plot of the CF lines. The possible accumulation of reaction products from the previous discharge pulses was taken into account by modeling a sequence of 3,000 pulses in each run (12 h of CPU time) while accounting for the loss of the products by convection in a flow of the buffer gas into the pump. The rates of reactions were adopted from the NIST database [21] and original literature (citations listed in Table 1).

The main mechanism of the dissociation of the molecules in the glow discharge is the collisions with free electrons generated by electron ionization and by Penning ionization. The rate constant of electron dissociation was calculated according to Morrison et al.: [40]

$$k(T_e) = \pi \left(\frac{e}{4\pi\varepsilon_0 E_A} \right)^2 \cdot \left(\frac{8eT_e}{\pi m_e} \right)^{1/2} \cdot \left(1 + \frac{2T_e}{E_A} \right) \exp(-E_A/T_e) \tag{7}$$

Here, e and m_e are the electronic charge and mass, ε_0 is the permittivity of the vacuum (all in SI units), E_A is the activation energy for dissociation in eV and T_e is the electron temperature expressed in eV.

Table 1 Reactions in the CF_3Br discharge and afterglow

No.	Dissociation reaction	Threshold energy (eV)	Ref.
D0	$CF_3Br + e^- \rightarrow CF_3 + e^- + Br$	2.60	[42, 43]
D1	$CF_2Br + e^- \rightarrow CF_2 + e^- + Br$	2.79	Estimated
D2	$CF_4 + e^- \rightarrow CF_3 + e^- + F$	5.31	[30]
D3	$CF_3 + e^- \rightarrow CF_2 + e^- + F$	3.94	[44]
D4	$CF_2 + e^- \rightarrow CF + e^- + F$	4.59	[30]
D5	$CF + e^- \rightarrow C + e^- + F$	5.60	Estimated
D6	$C_2F + e^- \rightarrow C + e^- + CF$	6.16	Estimated
D7	$C_2F_2 + e^- \rightarrow CF + e^- + CF$	5.76	[30]
D8	$C_2F_2 + e^- \rightarrow C_2F + e^- + F$	5.24	Estimated
D9	$C_2F_4 + e^- \rightarrow C_2F_3 + e^- + F$	5.11	Estimated
D10	$C_2F_6 + e^- \rightarrow C_2F_5 + e^- + F$	5.04	Estimated
D11	$C_2F_5 + e^- \rightarrow C_2F_4 + e^- + F$	4.95	Estimated
D12	$C_2F_3 + e^- \rightarrow C_2F_2 + e^- + F$	4.95	Estimated
D14	$C_2F_3 + e^- \rightarrow CF_2 + e^- + CF$	0.44	[45]
D15	$C_2F_4 + e^- \rightarrow 2\ CF_2 + e^-$	3.70	Estimated
D16	$C_2F_6 + e^- \rightarrow 2\ CF_3 + e^-$	3.32	Estimated
D17	$C_2F_5 + e^- \rightarrow CF_3 + e^- + CF_2$	0.44	[45]

No.	Radical–radical reaction	Rate constant (cm^3s^{-1})	Ref.
R0	$CF_3 + CF_3 \rightarrow C_2F_6$	5.25×10^{-12}	[46]
R1	$CF_3 + F \rightarrow CF_4$	4.40×10^{-11}	[47]
R2	$CF_3 + Br \rightarrow CF_3Br$	4.40×10^{-11}	Estimated using[47]
R3	$CF_2 + F \rightarrow CF_3$	4.30×10^{-14}	[48]
R4	$CF_3 + CF_2 \rightarrow C_2F_5$	8.80×10^{-13}	[48]
R5	$CF_2 + CF_2 \rightarrow C_2F_4$	4.01×10^{-14}	[49]
R6	$CF + F \rightarrow CF_2$	1.00×10^{-13}	[50]
R7	$CF_4 + F \rightarrow CF_3 + F_2$	4.15×10^{-15}	Estimated using[51]
R8	$CF_3 + F \rightarrow CF_2 + F_2$	4.15×10^{-15}	
R9	$CF_2 + F \rightarrow CF + F_2$	4.15×10^{-15}	
R10	$CF_3 + F_2 \rightarrow CF_4 + F$	7.00×10^{-14}	Estimated using[48]
R11	$CF_2 + F_2 \rightarrow CF_3 + F$	8.32×10^{-14}	[52]
R12	$CF + F_2 \rightarrow CF_2 + F$	8.32×10^{-14}	Estimated using[52]
R13	$C + F_2 \rightarrow CF + F$	8.32×10^{-14}	
R14	$CF_3 + CF_3 \rightarrow CF_4 + CF_2$	1.00×10^{-15}	
R15	$CF_3 + CF_2 \rightarrow CF_4 + CF$	1.00×10^{-15}	
R16	$CF_2 + CF_2 \rightarrow CF_3 + CF$	1.00×10^{-15}	
R17	$CF + CF_3 \rightarrow 2CF_2$	3.90×10^{-12}	[53]
R18	$CF_2 + CF \rightarrow C_2F_3$	1.00×10^{-12}	[47]
R19	$C_2F_3 + F \rightarrow C_2F_4$	5.00×10^{-14}	
R20	$C_2F_4 + F \rightarrow CF_3 + CF_2$	4.00×10^{-11}	
R21	$C_2F_5 + F \rightarrow 2\ CF_3$	1.00×10^{-11}	
R22	$C_2F_6 + F \rightarrow CF_3 + CF_4$	1.00×10^{-11}	

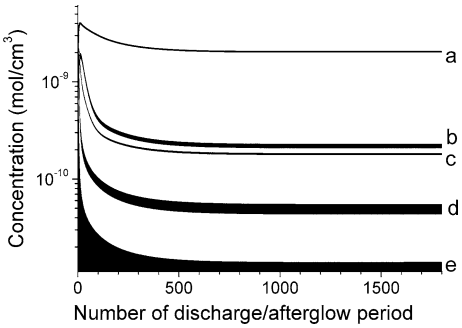

Fig. 6 Calculated time resolved concentration profiles of CF_4 (**a**), CF (**b**), CF_2 (**c**), CF_3Br (**d**) and CF_3 (**e**) in CF_3Br pulse discharge as a function of the number of discharge/afterglow periods

The results of this model applied to the CF_3Br discharge are summarized in Fig. 6. The system achieved the equilibrium between dissociation and recombination reactions after several thousand discharge/afterglow periods. The calculated concentration of CF_4 was higher than that of CF and CF_2, which is in agreement with the experimental data (see above). The concentrations of CF_3 and $C_xF_yBr_z$ species not observed by FTIR measurements were about two orders of magnitude lower than those of CF and CF_2. Both experimental and calculated data that predict a high concentration of CF are in agreement with the literature data of Kim et al. [41] for a CF_4 discharge. A similar model can be applied to the CF_3CFHCF_3 discharge.

Conclusion

The time-resolved emission spectra of CF_3Br and CF_3CFHCF_3 in helium discharge plasma were measured in the 600–6,000 cm^{-1} region using a high resolution Fourier transform spectrometer. The reaction mechanism that was suggested on the basis of time resolved data starts by Penning ionization and the reaction of precursors with excited helium atoms and/or fast electrons up to atoms and low molecular fragments. The major unstable products were CF_4, CF and CF_2, which is in agreement with a kinetic model. The formation of stable molecules and vibrational cooling to the ground state were observed in the range of tens of microseconds. All measurements show the formation of toxic and/or reactive stable products, e.g., HF, HBr, CO and HCN.

Acknowledgments This research was supported by the Academy of Sciences of the Czech Republic (Grants Nos. IAA 400400705 and IAAX 00100903), by the Ministry of Education, Youth and Sports of the Czech Republic via the projects OC09050 (in the frame of the COST ES0604 Action) and LD11012 (in the frame of the COST CM0901 Action) and by the Grant Agency of the Czech Republic (project no. P108/11/1312). The authors (V.N., P.B., E.G., M.S.) are grateful for the financial support via the project no. SP/2010148 funded in the frame of specific research by the Student Grant System (SGS) of the VŠB-Technical University of Ostrava.

References

1. Zurer PS (1993) Chem Eng News 71:12
2. Velders G, Madronich S, Clerbaux C, Derwent R, Grutter M, Hauglustaine D, Incecik S, Ko M, Libre J-M, Neilson O, Stordal F, Zhu T, Blake D, Cunnold D, Daniel J, Forster P, Fraser P, Krummel P, Manning A, Montzka S, Myhre G, O'Doherty S, Oram D, Parther M, Prinn R, Reimann S, Simmonds P, Wallington T, Weiss R (2005) Chemical and Radiative Effects of Halocarbons and Their Replacement

Compounds. IPCC/TEAP Special Report on Safeguarding the Ozone Layer and the Global Climate System: Issues Related to Hydrofluorocarbons and Perfluorocarbons, IPCC Working Group I & III and TEAP. Cambridge University Press, Cambridge, UK
3. Murphy AB, Farmer AJD, Horrigan EC, McAllister T (2002) Plasma Chem Plasma Process 22:371
4. Takigami H, Suzuki G, Hirai Y, Sakai S-i (2009) Chemosphere 76:270
5. Windham GC, Pinney SM, Sjodin A, Lum R, Jones RS, Needham LL, Biro FM, Hiatt RA, Kushi LH (2010) Environ Res 110:251
6. Zegers EJP, Williams BA, Fisher EM, Fleming JW, Sheinson RS (2000) Combust. Flame 121:471
7. Bailleux S, Dréan P, Godon M, Zelinger Z, Duan C (2004) Phys Chem Chem Phys 6:3049
8. Bailleux S, Dréan P, Zelinger Z, Civiš S, Ozeki H, Saito S (2005) J Chem Phys 122:1
9. Bailleux S, Dréan P, Zelinger Z, Godon M (2005) J Mol Spectrosc 229:140
10. Zelinger Z, Dréan P, Walters A, Avilès JR, Bogey M, Pernice H, Von Ahsen S, Willner H, Breidung J, Thiel W, Bürger H (2003) J Chem Phys 118:1214
11. Civiš S, Kubát P, Nishida S, Kawaguchi K (2006) Chem Phys Lett 418:448
12. Civiš S, Šedivcová-Uhlíková T, Kubelík P, Kawaguchi K (2008) J Mol Spectrosc 250:20
13. Civiš S, Matulková I, Cihelka J, Kawaguchi K, Chernov VE, Buslov EY (2010) Phys Rev A. 81
14. Kawaguchi K, Sanechika N, Nishimura Y, Fujimori R, Oka TN, Hirahara Y, Jaman AI, Civiš S (2008) Chem Phys Lett 463:38
15. Jonkers J, Van Der Mullen JAM (1999) J Quant Spectrosc Rad Transfer 61:703
16. Schaepkens M, Standaert TEFM, Rueger NR, Sebel PGM, Oehrlein GS, Cook JM (1999) J Vac Sci Technol A 17:26
17. Chang MB, Chang J-S (2006) Ind Eng Chem Res 45:4101
18. Modiano SH, McNesby KL, Marsh PE, Bolt W, Herud C (1996) Appl Opt 35:4004
19. Kawaguchi K, Hama Y, Nishida S (2005) J Mol Spectrosc 232:1
20. Alexandrov VM, Flender U, Kolokolov NB, Rykova OV, Wiesemann K (1996) Plasma Sources Sci Technol 5:523
21. NIST (2010) in NIST database, URL: http://webbook.nist.gov/chemistry/ downloaded 3 Nov 2010
22. Nakanaga T, Ito F, Takeo H (1994) J Mol Spectrosc 165:88
23. Burkholder JB, Howard CJ, Hamilton PA (1988) J Mol Spectrosc 127:362
24. Gabriel O, Stepanov S, Pfafferott M, Meichsner J (2006) Plasma Sources Sci Technol 15:858
25. Yamada C, Hirota E (1983) J Chem Phys 78:1703
26. Copeland G, Lee EPF, Dyke JM, Chow WK, Mok DKW, Chau FT (2010) J Phys Chem A 114:3540
27. Bell KL, Dalgarno A, Kingston AE (1968) J Phys B 1:18
28. Tokue I, Sakai Y, Yamasaki K (1996) J Chem Phys 106:4491
29. Blanksby SJ, Ellison GB (2003) Acc Chem Res 36:255
30. Modica AP, Sillers SJ (1968) J Chem Phys 48:3290
31. Modica AP (1966) J Chem Phys 44:1585
32. Hildenbrand DL (1975) Chem Phys Lett 32:523
33. Nakano T, Sugai H (1992) Jpn J Appl Phys 31:2919
34. Goto M, Nakamura K, Toyoda H, Sugai H (1994) Jpn J Appl Phys 33:3602
35. Ferus M, Kubelík P, Kawaguchi K, Dryahina K, Španěl P, Civiš S (2011) J Phys Chem A. (in press)
36. http://numpy.org/ downloaded 25 Oct 2010
37. URL: http://scipy.org/, downloaded 25 Oct 2010
38. Corbella C, Polo MC, Oncins G, Pascual E, Andujar JL, Bertran E (2005) Thin Solid Films 482:172
39. Winchester MR, Payling R (2004) Spectrochim Acta B 59:607
40. Morrison NA, William C, Milne WI (2003) J Appl Phys 94:7031
41. Kim JH, Chung KH, Yoo YS (2005) J Korean Phys Soc 47:249
42. Hidaka Y, Nakamura T, Kawano H (1989) Chem Phys Lett 154:573
43. Hidaka Y, Nakamura T, Kawano H, Koike T (1993) Int J Chem Kinet 25:983
44. Srinivasan NK, Su MC, Michael JV, Jasper AW, Klippenstein SJ, Harding LB (2008) J Phys Chem. A 112:31
45. Li K, Kennedy EM, Dlugogorski BZ (2000) Chem Eng Sci 55:4067
46. Geigl M, Peters S, Gabriel O, Krames B, Meichsner J (2005) Contrib Plasma Phys 45:369
47. Ryan KR, Plumb IC (1986) Plasma Chem Plasma Process 6:231
48. Plumb IC, Ryan KR (1986) Plasma Chem Plasma Process 6:205
49. BattinLeclerc F, Smith AP, Hayman GD, Murrells TP (1996) J Chem Soc-Faraday Trans 92:3305
50. Vanhoeymissen J, Deboelpaep I, Uten W, Peeters J (1994) J Phys Chem 98:3725
51. Westbrook CK (1983) Combust Sci.Technol 34:201
52. Seeger C, Rotzoll G, Lubbert A, Schugerl K (1982) Int J Chem Kinet 14:457
53. Peeters J, Vanhoeymissen J, Vanhaelemeersch S, Vermeylen D (1992) J Phys Chem 96:1257